Molecular dynamics at constant temperature and pressure

S. Toxvaerd
Department of Chemistry, H. C. Ørsted Institute, University of Copenhagen, Universitetsparken 5, DK-2100 Copenhagen Ø, Denmark
(Received 6 July 1992)

Algorithms for molecular dynamics (MD) at constant temperature and pressure are investigated. The ability to remain in a regular orbit in an intermittent chaotic regime is used as a criterion for long-time stability. A simple time-centered algorithm (leap frog) is found to be the most stable of the commonly used algorithms in MD. A model of N one-dimensional dimers with a double-well intramolecular potential, for which the distribution functions at constant temperature T and pressure P can be calculated, is used to investigate MD-NPT dynamics. A time-centered NPT algorithm is found to sample correctly and to be very robust with respect to volume scaling.

PACS number(s): 61.20.Ja, 05.20.Gg, 02.70.−c, 05.45.+b

I. INTRODUCTION

The time evolution of a complex N-body system can be simulated using the molecular-dynamics (MD) technique, where the classical mechanical equations of motion are integrated [1–2]. However, since the motions of the individual subsystems are by nature chaotic, it is, in general, of little relevance to try to solve the individual equations accurately and the criteria an MD simulation must fulfill is that it scans the phase space dynamically correctly. Recently a series of investigations [3–5] indicates that, although an MD algorithm results in noisy trajectories due to numerical inaccuracy, some true trajectories remain close to the noisy one for long times. It is explained [4] in that the discrete mapping describes the exact time evolution of a slightly perturbed Hamiltonian system and thus possesses the perturbed Hamiltonian as a conserved quantity. It is, however, only true for symplectic integrators [3–8] which conserve the phase space and ensure time reversibility. Thus the individual trajectories should only be considered as "representative" from which the ensemble behavior is obtained by averaging. Basically the MD simulation of N objects samples from a microcanonical ensemble of constant energy, but during the past decade, a series of other MD ensemble simulations have been developed, among which the canonical simulation is the most commonly used.

The investigations of symplectic integrators have resulted in a series of higher-order explicit and implicit algorithms [4,6–8]. The particle motions in an MD simulation are, however, generally obtained by simple finite-difference algorithms due to the (computer) time-consuming MD simulations. One of the most frequently used algorithms is a centered-difference Stoermer algorithm, which in MD is named the Verlet algorithm—or leap-frog algorithm. Another algorithm used in MD is a simplified version of Gear's iterative corrector scheme for stiff differential equations. Also used, but more rarely, is the Runge-Kutta algorithm.

A criterion an MD algorithm must fulfill is that it scans the relevant phase space correctly, leading to the correct equilibrium properties and (linear-) response regime. However, since the exact functions are usually not known even for simple statistical models, one needs some other criterion for an accurate test of different MD algorithms such as time reversibility and symplectic integration [5–7]. The Verlet algorithm, and its analogy, the leap-frog algorithm, are both time reversible and symplectic [5] and one might think that the two criteria are identical. This is, however, not the case for constrained dynamics as will be demonstrated. Neither the Gear nor the Runge-Kutta algorithm, presently used in MD, are time reversible or symplectic [9]. These higher-order algorithms will in general follow the analytic solution of the differential equations a little bit longer and better than a simpler version, but they suffer from a drift in the observed mean quantities, such as the mean energy, due to the broken time symmetry and nonsymplectic behavior. This article deals with MD ensemble simulations. For accurate numerical integration of the equation of motion of celestial mechanics see also Ref. [10].

The different MD-ensemble simulations are performed by introducing new differential equations [11] which couple, e.g., Hamilton's equations to various heat baths, pressure controller, etc. The corresponding dynamical equations are still time reversible, and it is possible to formulate simple, reversible finite-difference algorithms [12–13]; but the symplectic behavior is only obtained in mean, since the different ensemble averages are achieved by a "reversible shaking" of the phase space.

In order to perform a precise investigation of the influence of various sources of errors and algorithm defects on MD, we need to examine systems for which exact solutions exist. The (Boltzmann) partition function for a simple canonical (N,V,T) ensemble can be calculated easily, and it is also possible to construct constant pressure (N,P,T) systems for which the equation of state and the partition functions can be calculated with a high degree of accuracy [14]. These circumstances are used to investigate the sensitivity of MD simulations to various algorithm defects and numerical errors and inaccuracy.

II. MOLECULAR DYNAMICS AT CONSTANT TEMPERATURE

The stability of an MD algorithm is, in the present investigation, determined by its ability to maintain a regular orbit in the phase space for a system with intermittent chaos. It is well know that simple driven pendulum systems can exhibit intermittent chaotic behavior. Thus, by choosing a condition for which the system still behaves regularly, but where it behaves chaotically for a small change of the dynamics, we achieve a sensitive measure of the stability of an algorithm, and the influence of various numerical errors on the integrator.

The canonical MD simulations are obtained by the Nosé-Hoover (NH) technique [11] and its extension [15]. The Hamilton's equations for an N-particle system with potential energy $U(\mathbf{q}^N)$

$$\dot{q}=\frac{p_i}{m_i} , \tag{1a}$$

$$\dot{p}_i=f_i-\eta p_i , \tag{1b}$$

are constrained with a time dependent friction η

$$\dot{\eta}=\left[\sum_i \frac{p_i^2}{m_i}-gkT\right]\Big/(gkT\tau_\eta^2) , \tag{2}$$

which varies in time with the total excess of kinetic energy to its canonical mean value for a system of g degrees of freedom and governs by a characteristic thermostat relaxation time τ_η. It is easy to derive simple time-centered finite-difference algorithms for these equations [12,13], which ensures time reversibility; but Eq. (2) results in equations which are only symplectic in the mean. For simple systems such as harmonic oscillators or a double-well potential the dynamics can be regular [5,16]. We have analyzed the dynamics for the two double wells shown in Fig. 1. There are several reasons for this choice of potentials. Simple systems with these intramolecular potentials exhibit intermittent chaotic behavior and Friedman and Auerbach [5] have investigated the micro-

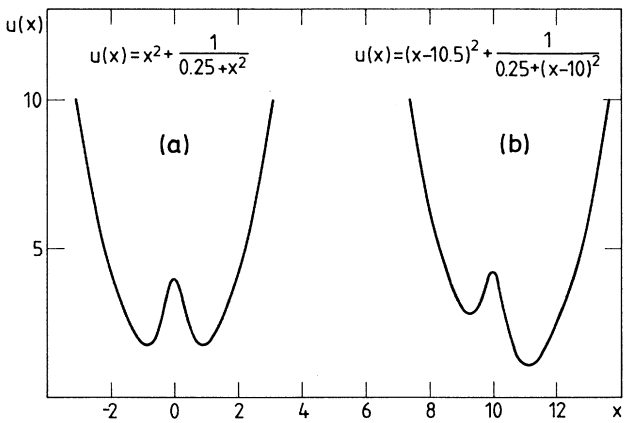

FIG. 1. The two intramolecular potentials, used in the MD calculations. The extremes are (a) $(\pm\sqrt{3}/2, 1.75)$, (0.4); (b) (9.28,2.79), (9.97,4.27), (11.06,1.04).

canonical dynamics in a double well and found numerical introduced stochasticity. Finally we notice that it is easy to construct simple nontrivial systems of dimers and polymers with intramolecular double-well potentials, where the partition function and distribution functions can be calculated accurately [14] for the (N,P,T) ensemble.

The symplectic behavior of an algorithm is achieved by demanding the Jacobian to be unity for the (discrete) transformation of variables $\mathbf{q}^N(t),\mathbf{p}^N(t)\rightarrow\mathbf{q}^N(t+h)$, $\mathbf{p}^N(t+h)$ of the N particles from time t to $t+h$. In the case of the simple time-centered algorithm Hamilton's equations leads to the reversible time propagator

$$\frac{q_i(t+h)-q_i(t)}{h}=p_i(t+h/2)/m_i , \tag{3a}$$

$$\frac{p_i(t+h/2)-p_i(t-h/2)}{h}=f_i(t) , \tag{3b}$$

which in MD is called the leap-frog algorithm. If we instead consider Newton's equations the time-centered algorithm for the second-order differential equations is

$$q_i(t+h)=2q_i(t)-q_i(t-h)+h^2\frac{f_i(t)}{m_i} . \tag{4}$$

By inserting (3b) in (3a) one obtains (4) so Eqs. (3) and (4) are identical and the two classical mechanical formulations are maintained in the simple time-centered formulations and (4) shows that the dynamics takes place (e.g.) in the $\mathbf{q}^N$ space with momentum as a dummy variable and, from (3) that $\mathbf{q}^N$ and $\mathbf{p}^N$ are not known at the same time, all in close analogy to quantum mechanics.

It is easy [5] to calculate the Jacobian for the nth step for the leap-frog algorithm (3)

$$J_n\equiv\frac{\partial(q_{n+1}^N,p_{n+1}^N)}{\partial(q_n^N,p_n^N)}=1 \tag{5}$$

so the simple time-centered propagator(s) maintains not only the time reversibility but also the symplectic behavior of classical mechanics. However, from a numerical point of view Eq. (3) is to be preferred since the roundoff errors are less important in this version of classical dynamics. The integrator (3) or (4) appears under different names in the MD literature: Leap frog, Verlet [17], Stoermer, Beeman [18], velocity Verlet [19], and recently, position Verlet [20]. They all generate identical trajectories except for numerical roundoff errors and thus they have the same quality with respect to energy conservation.

When the classical dynamics is coupled to an NH heat bath the reversibility is maintained, but not the symplectic behavior. No Hamiltonian exists for the system, but

$$H=\sum_i^N \frac{p_i^2}{2m_i}+U_N(q^N)+gkT\int_0^t\eta(\tau)d\tau +\eta(t)^2gkT\tau_\eta^2/2 \tag{6}$$

remains a constant of the motion. Both the differential equations (1) and (2) and its time-centered formulations [12,13] are not symplectic. The Jacobian transformation for the leap-frog propagator is

$$J_n=\frac{\partial(q^N_{n+1},q^N_{n+1},\eta_{n+1})}{\partial(q^N_n,p^N_n,\eta_n)}$$
$$=\frac{1-\frac{h}{2}\eta(t_n)}{1+\frac{h}{2}\eta(t_n+h)}\ , \tag{7}$$

so the single discrete steps are not volume conserving. However, since the thermostat variable η for time-centered algorithms is Gaussian distributed with $\langle\eta(t)\rangle=0$, the total Jacobian

$$J=\prod_n J_n \tag{8}$$

fluctuates around unity.

The NH dynamics of a single oscillator with the double-well potential (Fig. 1) [5]

$$u(x)=x^2+\frac{1}{0.25+x^2}\ , \tag{9}$$

examined by Friedman and Auerbach, were calculated for various algorithms. The dynamics exhibit intermittent chaotic behavior depending on the thermostat parameter τ_η and temperature T. One regular orbit for $\tau_n\approx 0.1$ and $kT/\varepsilon=2$ was used for the test of stability of various MD time propagators. For slightly larger τ_η the system behaved chaotically, but the algorithms remain in the regular orbit for (very) small and discrete time intervals h and for τ_η up to 0.110 26. Table I gives the results for the time increment $h=0.001$, which should be compared with the time required for the oscillation to complete a full circle which is $\tau=6.57$ [21].

The second column in Table I gives the time $\mathcal{T}$ the integrators remain in the regular orbit before they jump into the chaotic regime. The next column shows the mean deviation from the pseudo-Hamiltonian Eq. (6). The systems are started at $x=0$ and for $H_0=4$, and the averages are for 10^7 time steps. The fourth column gives the mean deviation $|\Delta H|$ per step, and column five shows the mean friction. The last column shows the mean Jacobian, Eq. (8) of the discrete integration. The fifth-order predictor-(pseudo-) corrector Gear algorithm, most commonly used in MD, deviates from the other one by being the worst to remain in the regular orbit and by having a drift in the integrator, enough to drive it into the chaotic regime. This shortcoming of the Gear algorithm is also known for other systems [22].

None of the integrators showed any strong nonsymplectic behavior. The classic fourth-order Runge-Kutta is nearly symplectic with the smallest drift in H and η, but does not remain in the regular solution as long as do the simple time-centered third-order predictors (with a time step $h=10^{-4}$ it remains in the regular orbit as long as the others and with a perfectly conserved H and $\langle\eta\rangle=0$). However, this (kind of) algorithm is not suited for routine MD of complex systems because one has to perform the (computer) time-consuming force calculations four times per step.

The two versions of simple time-centered predictors derived in Refs. [12] and [13] follow the regular orbit for the longest time. In the case of the leap-frog integrator the chaotic behavior first appeared after 771 cycles in the regular orbit. One remarkable property of the integrators is that the roundoff errors do not play a significant role for the introduced chaos. A single-precision version of the Verlet algorithm does not deviate significantly in the quality of integration from its double-precision version. Since some (super-) computers run with double speed in single precision, one can save a factor 2. We notice that there is no documentation in the literature for the necessity of performing the calculations in double precision in MD.

Poincaré maps (PM's) of sections p vs η at $x=0$ are shown in Figs. 2 and 3. Figure 2(a) is the PM for the Runge-Kutta integrator and for the 141 times it maintained in the regular orbit, and Fig. 2(b) is the corresponding PM for the leap-frog integrator obtained from the 771 loops. A representative PM for the time after the Runge-Kutta integrator left the regular orbit is shown in Fig. 3. As indicated from the figure the dynamics is still not fully chaotic. The distribution of dots shows structures with a PM dimension of less than 2.

The lack of full chaotic behavior can be shown simply by plotting the energy distribution which for a fully chaotic system should be Boltzmann distributed. This is demonstrated in Fig. 4, which shows a (high-) temperature state $kT/\varepsilon=4$ with no regular trajectories. The dotted line in the upper part (a) of Fig 4 gives the distribution $P(x)$ for the Verlet algorithm [12] after 10^7 integration steps together with the Boltzmann distribution in the solid line. As can be seen from the figure, the lack of full chaotic behavior also appears in the energy distribution

TABLE I. Integration of a regular orbit with various MD algorithms at constant temperature $kT/\varepsilon=2$, a time increment $h=10^{-3}$, and a thermostat relaxation time $\tau_\eta=0.110\,26$.

Algorithm	$\mathcal{T}$	$\langle H\rangle-H_0$	$\langle\lvert\Delta H\rvert\rangle$	$\langle\eta\rangle$	J
Five-pc Gear	839	1.2×10^{-2}	8.2×10^{-5}	-6.65×10^{-4}	1.942
Fourth order Runge-Kutta	928	0.4×10^{-5}	7.8×10^{-5}	-1.67×10^{-5}	1.182
Verlet single precision[a]	2411	4.6×10^{-5}	7.8×10^{-5}	5.72×10^{-5}	0.453
Verlet[a]	2711	4.6×10^{-5}	7.8×10^{-5}	4.71×10^{-5}	0.625
Leap frog[b]	5068	3.1×10^{-5}	8.0×10^{-5}	9.06×10^{-5}	0.404

[a] Reference [12].
[b] Reference [13].

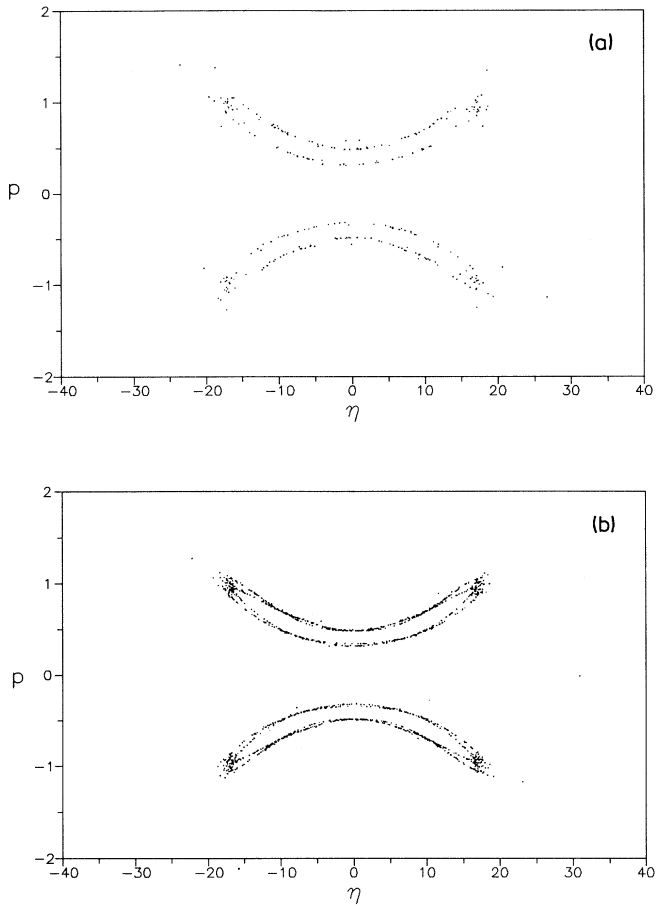

FIG. 2. Poincaré maps of momentum p vs friction η for $x=0$ at $T=2$ and $\tau_\eta=0.110\,26$ and for the regular trajectory at the start of the integration. (a) The fourth order Runge-Kutta integrator which maintained in the regular solution 144 full circles. (b) Leap-frog integrator and for 771 full circles.

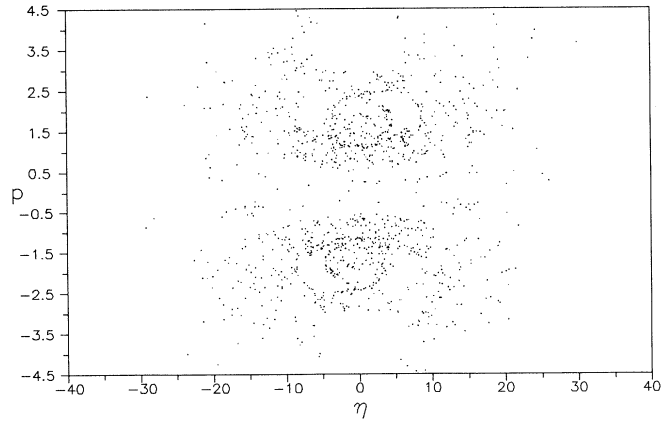

FIG. 3. Poincaré map of the chaotic part of the trajectory and for the fourth-order Runge-Kutta integrator.

which shows some pattern in the deviation from the Boltzmann distribution $\exp[-\beta u(x)]$.

The ergodic behavior can be achieved by extending the Nosé-Hoover dynamics in the way proposed by Bulgac and Kusnezov (BK) [15]. It is, however, in general not possible to construct time-reversible centered difference algorithms for the BK thermostats, but it can be derived easily for linear frictions (see the Appendix). If one, for example, introduces a friction in the q space by modifying (1a) to

$$\dot{q}_i=\frac{p_i}{m_i}-\xi q_i \tag{10}$$

with a ξ-friction dynamics given by [15]

$$\dot{\xi}=-\left[\sum_i f_i q_i+gkT\right]\Big/(gkT\tau_\xi^2)\ , \tag{11}$$

the corresponding dynamics is fully chaotic. The dots in Fig. 4(a) show a perfect Boltzmann distribution and in Fig. 4(b) we have shown a log-log plot of the integrated square of the deviation from $\exp[-\beta u(x)]$ as a function of the numbers N of integration steps. The dots and the solid line are for the BK thermostat, whereas the crosses

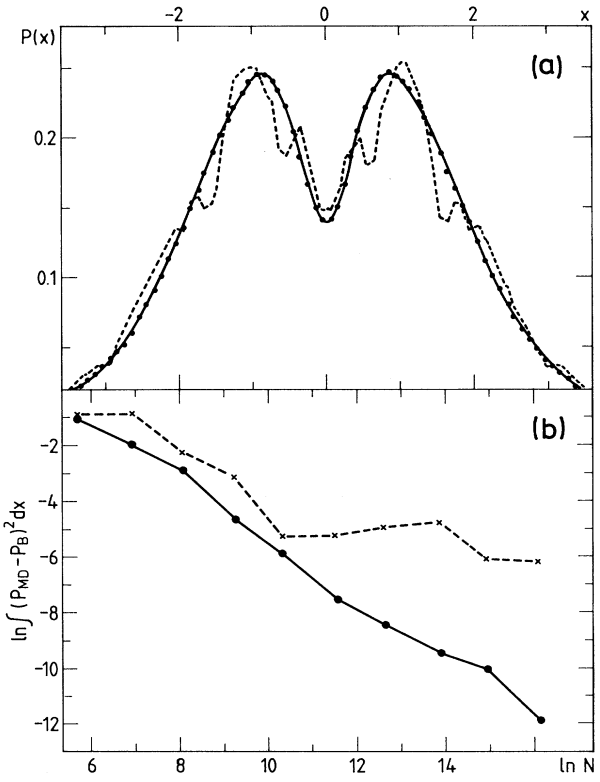

FIG. 4. (a) Energy distributions at $T=4$. The solid line is the canonical Boltzmann distribution and the dotted line is the NH result of 10^7 time steps with $h=10^{-2}$ and $\tau_\eta=0.15$. The full circles give the corresponding BK thermostated values with $\tau_\xi=1$. (b) Log-log plot of the integral of the square of the deviation from the Boltzmann distribution. The crosses and the dotted line are for the NH thermostat, and the solid points and solid line are for the BK thermostat.

and the dotted line are for the NH dynamics. As can be seen from the figure, the distribution is not essentially improved after the first 2.5×10^4 time steps in the case of NH dynamics, whereas the distribution converges monotonically towards the Boltzmann distribution by using BK dynamics and using the algorithms in the Appendix. The result is in agreement with a corresponding analysis by Bulgac and Kusnezov [23].

To conclude this part of the investigation the computations demonstrate the importance of time reversibility in the MD dynamics. An algorithm like the Gear algorithm, which is constructed for numerical solutions to analytic, stiff differential equations is not suitable for MD, since it is either much too costly or, in its simple version, used in MD systematically wrong. Neither does the numerical accuracy of the dynamics plays a significant role. There is no difference in the result obtained either by performing the dynamics either in single or double precision. These results are due to the chaotic nature of the classical dynamics. However, if the system is not fully chaotic, the Boltzmann distribution can be obtained by extending the dynamics in the way proposed by Bulgac and Kusnezov [15].

III. MOLECULAR DYNAMICS AT CONSTANT PRESSURE

The MD simulations for N molecules at constant temperature T and pressure P, (N,P,T), are performed by scaling the volume and using the virial of the intermolecular forces to calculate the pressure. In the past this was done in a rather *ad hoc* manner; but with the derivation of the NH dynamics the procedure can be made more rigorous by introducing a pressure thermostat with the friction $\zeta(t)$. The "Verlet" time-centered finite-difference algorithm for the (N,P,T) MD is derived in Ref. [12]. The corresponding reversible leap-frog version is given in the Appendix. Again we notice that the dynamics are no longer strictly symplectic, but still time reversible.

The analysis of (N,P,T) ensemble simulations is difficult since the exact results are in general not known. The investigations are limited to what can be characterized as "stability tests" of the (N,P,T) algorithms and by comparing the mean results with corresponding data for other ensembles. It is, however, possible to construct a simple (N,P,T) system where the configurational integral and the distribution functions can be calculated. The present system is a one-dimensional string of dimers with an intramolecular two-state potential given in Fig. 1(b). Although the system is too complicated to formulate the equation of state and the distribution functions in terms of known analytic functions, its statistical mechanics can easily be calculated numerically with a high degree of accuracy.

The general derivation of the equation of state for N one-dimensional molecules in the volume L is given in Ref. [14]. The present molecules deviate from the molecules considered by Hornell and Halls by also having an intermolecular potential u_{inter} and by using periodical boundaries at $x=0$ and L in order to avoid wall effects. The molecules have hard cores (u_{inter} and u_{intra}) so the classical configurational integral Z is a convolution. Since the (N,P,T) configurational integral Y, with the (additional) $\exp(-\beta PL)$ factor is just the Laplace transform of Z with βP as the Laplace variable, the (NPT) configurational integral Y is a product of the Laplace transform of the individual Boltzmann factors. For N dimers with an intra- and (short-range) intermolecular potential Y is

$$Y=\frac{\lambda}{\Lambda^{2N}}(f_{\text{intra}}f_{\text{inter}})^N \tag{12}$$

with

$$f_i=\int_0^\infty \exp\{-\beta[Px+u_i(x)]\}dx \ . \tag{13}$$

The (NPT) mean volume $\langle L\rangle$ is obtained from the thermodynamic relation and (12) and (13)

$$\langle L\rangle=-\beta\left[\frac{\partial \ln Y}{\partial P}\right]_{N,\beta}=N[\langle l_{\text{inter}}\rangle+\langle l_{\text{intra}}\rangle] \ , \tag{14}$$

with

$$\langle l_{\text{intra}}\rangle\frac{\int_0^\infty \exp\{-\beta[Px+u_{\text{intra}}(x)]\}x\,dx}{\int_0^\infty \exp\{-\beta[Px+u_{\text{intra}}(x)]\}dx} \ . \tag{15}$$

The mean intramolecular bond length at constant pressure $P=P_{\text{eq}}$ and temperature T can be calculated from (15) with great accuracy. Isotherms of $\langle 1_{\text{intra}}(P)\rangle$ and for the potential in Fig. 1(b) are shown in Fig. 5. The in-

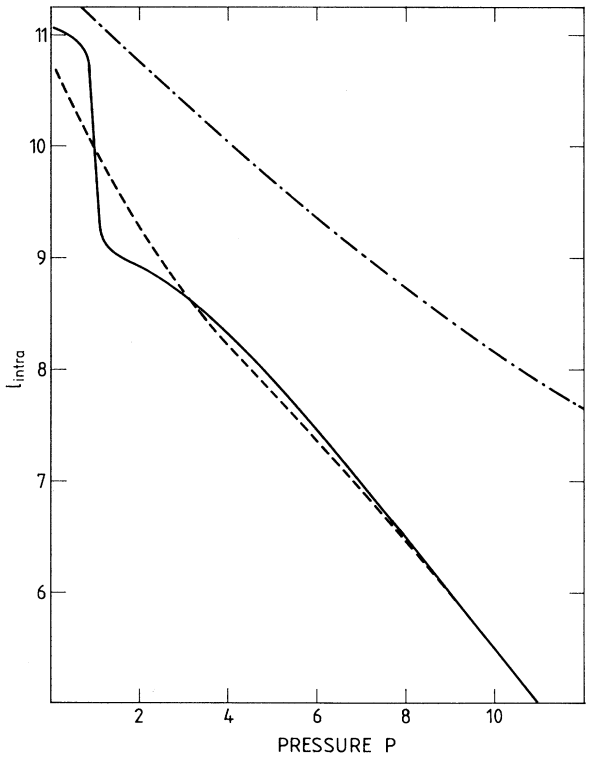

FIG. 5. Isotherms for the intramolecular bond length l_{intra} as a function of the pressure P, obtained by Eq. (15). Full curve is for $T=0.01$; dashed line is for $T=2$; and dash-dotted line is for $T=100$.

tramolecular potential is modified from its symmetrical version in Fig. 1(a) for several reasons. We want to analyze constant pressure MD for its capability of equilibrium sampling and the unsymmetrical potential ensures a system with different inter- and intramolecular relaxation times. For the intermolecular molecular potential we have chose repulsive Lennard-Jones potentials and length and energies are given in units of its potential parameters σ and ε. It is, as mentioned, necessary for the "convolution technique" that the particles (monomers) have a given order and for the derivation of (14) that the monomer units in the dimers only interact with neighboring monomers. For this reason the minima positions in u_{intra} are shifted to a position for which both conditions are fulfilled for all points of states shown in Fig. 5. The system is a fluid (gas) for all points of state and with no phase transitions. The intramolecular thermal expansion coefficient

$$\alpha_{P,\text{intra}}=\frac{1}{l_{\text{intra}}}\left[\frac{\partial l_{\text{intra}}}{\partial T}\right]_P \tag{16}$$

is negative in some (T,P) areas due to the shift in population of the two intramolecular minima. This behavior is also found in another one-dimensional model [24]. However, $\alpha_{p,\text{intra}}$ is (very) small at $T\approx 1$, as can be seen from the figure, compared to the intramolecular compressibility

$$\beta_{T,\text{intra}}=-\frac{1}{l_{\text{intra}}}\left[\frac{\partial l_{\text{intra}}}{\partial P}\right]_T . \tag{17}$$

The consequence of this fact for MD *NPT* dynamics is that the thermodynamics of the system is more sensitive to the pressure thermostat than to the temperature thermostat. In other words, if the T thermostat does not sample correctly and gives a slightly wrong mean temperature, the impact on the thermodynamics is small compared to the impact from a corresponding shortcoming of constant pressure sampling due to the incompressibility of dense fluids.

An MD *NPT* system was set up with $N=200$ dimers interacting with the intramolecular potential in Fig. 1(b) and with repulsive Lennard-Jones potentials between intermolecular neighboring monomer units. The algorithm used for the integration is given in the Appendix. This time only the centered leap-frog version was used, since the conclusion from the canonical dynamics is that it is the best and most stable algorithm for generating the dynamics of chaotic systems. The equations of motion were integrated with a small time increment $h=0.001$, and for various values of τ_ζ. The MD results (○) at $T=2$ are shown in Fig. 6(a) together with the exact isotherm (dashed line). The results are for 10^5 time steps, and the MD obtained mean bond lengths converge monotonically towards the exact value with the increased integration time. The points connected with the straight lines and with the ordinate unit to the right show the deviation from the exact results. Bearing in mind that T and P are in units of the intermolecular potential parameters the isotherm $T=2$, and with P varying a decade is representative for MD simulations of fluids.

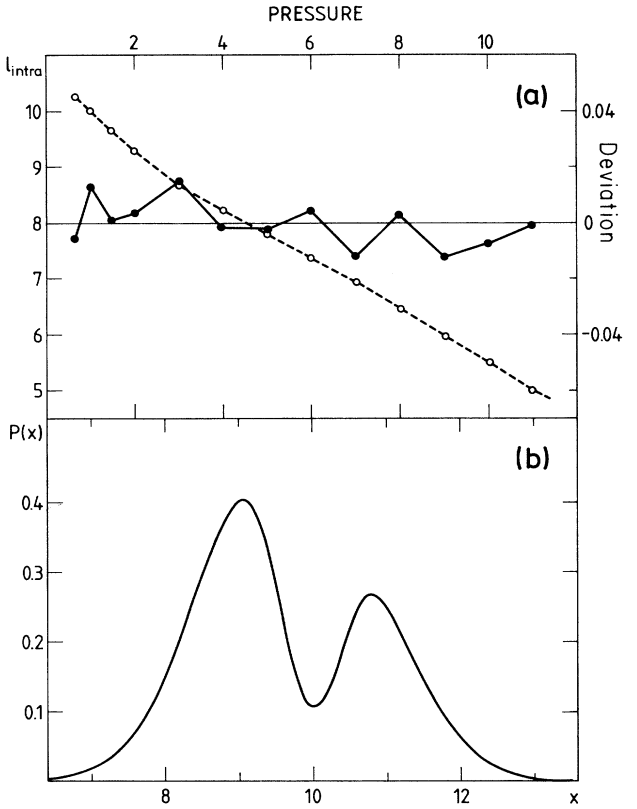

FIG. 6. (a) The exact isotherm $l_{\text{intra}}(P)$ at $T=2$ from Fig. 5 and with the MD determined points (○) included. Also shown with the ordinate unit to the right is the deviation $l_{\text{intra}}(\text{MD})-l_{\text{intra}}(\text{exact})$. (b) The probability distribution $P(x)$ of l_{intra} for $T=2$, and $P=1.47$. The MD obtained distribution is for 10^6 steps with $h=10^{-3}$.

In Fig. 6(b) the *NPT* ensemble distribution (15) at $T=2$ and $P=1.47$ is shown. This state was chosen for further investigation. The figure gives the exact distribution $[P(x)]_{\text{exact}}$ as well as the MD result of 10^6 time steps which only deviates with an integrated square deviation

$$\int_0^\infty [P_{\text{MD}}(x)-P_{\text{exact}}(x)]^2 dx = 1.09\times 10^{-5} , \tag{18}$$

not visible on the figure. As in the case of canonical sampling, double-precision dynamics are of no importance. The corresponding single-precision dynamics also converges monotonically towards the *NPT* distribution and with an integrated square deviation 1.5×10^{-5} for 10^6 steps at the same T,P point as (18). The mean collision time at this point of state is $\tau_{\text{coll}}=1.78$ and the mean time τ_{intra} a dimer stays in (or near) one of its two energy minima is $\tau_{\text{intra}}=5.75$. The fundamental problem in MD *NPT* sampling is how fast can one rescale the volume [25]. One would think that since these two times express the speed by which excess of inter- (intra-) molecular energy is dissipated in the ensemble, the pressure thermostat should be damped with a τ_ζ [in (A3)] bigger than these two times. This is, however, not the case. The thermostat functions even for much smaller τ_ζ values at the state $T=2, P=1.47$ down to $\tau_\zeta\approx 0.065$. The only minor

shortcoming in the dynamic sampling is a small deviation between the atomic and molecular temperature at high pressures, but as mentioned (16), the impact on the thermodynamics of this defect is small.

The dynamics of the present system of dimers is ergodic and fully chaotic, even at low temperatures ($T=0.01$) and for attractive Lennard-Jones potentials between the molecules. However, a line of one-dimensional subsystems interacting through anharmonic forces will at sufficiently low temperatures exhibit nonergodic behavior [26]. For this reason the q-space thermostat (10) was included in the investigation of MD *NPT* dynamics, but with no effect on the convergence of the sampling, measured by the integrated mean-square deviation (18). Finally it should be noticed that the virial of the intermolecular forces is rescaled to give the $P_{\rm eq}$ by rescaling the mass centers of the molecules and not the atomic centres, if not the thermostat fails for $\tau_\zeta < \tau_{\zeta\rm intra}$.

IV. CONCLUSION

The requirement of time-reversible and symplectic dynamics of classical, mechanical systems can be achieved by using simple time-centered finite-difference algorithms. They give "representative" trajectories and lead to a correct dynamical scanning of the microcanonical phase space, as opposed to nonsymplectic algorithms [3,4]. For other phase-space dynamics such as canonical dynamics or dynamical sampling at constant pressure, the differential equations are no longer symplectic, but it is still possible to formulate simple reversible (time-centered) algorithms both in Newton's formulations as well as for Hamilton's equations (leap frog).

The canonical dynamics of simple systems exhibit intermittent chaotic behavior and by choosing a regular solution close to a chaotic region one obtains a sensitive measure of stability for different algorithms. Furthermore, the double-well system is known to be sensitive to numerical roundoff errors which can drive a regular system into numerical introduced stochastic behavior [5]. The simple time-centered algorithms (Verlet, leap frog) are the best at remaining in the regular trajectory as opposed to the simple version of the Gear algorithms for stiff differential equations, often used in MD. Numerical accuracy of the MD arithmetic, however, plays an insignificant role, compared with the accuracy of the integration, since the same mean behavior, as well as the persistency to remain in the regular orbit is independent of whether the calculations are performed in single or double precision. However, if the system is not ergodic, it can easily be overcome by introducing a second thermostat as proposed in Ref. [15].

The constant pressure thermostat for a system, for which the equilibrium statistical mechanics can be calculated, works excellently and appears to be remarkably robust with respect to the speed by which the space is rescaled to give constant pressure.

ACKNOWLEDGMENTS

The author is grateful to Dr. H. Posch for drawing his attention to the non-symplectic behavior of HN dynamics and to Dr. W. G. Hoover for information about Refs. [3] and [4]. Helpful discussions with Dr. O.H. Olsen is gratefully acknowledged. Grant No. 11-7785 from the Danish Natural Science Research Council is gratefully acknowledged.

APPENDIX: TIME-REVERSIBLE, CENTERED-DIFFERENCE ALGORITHMS

An example of the canonical dynamics proposed by Bulgac and Kusnezov [15] is

$$\begin{aligned}
\dot{\mathbf{q}}_i &= \frac{\mathbf{p}_i}{m_i} - \xi \mathbf{q}_i \ , \\
\dot{\mathbf{p}}_i &= \mathbf{f}_i - \eta \mathbf{p}_i \ , \\
\dot{\xi} &= -\left[\sum_i \mathbf{f}_i \mathbf{q}_i + gkT\right] \Big/ (gkT\tau_\xi^2) \ , \\
\dot{\eta} &= \left[\sum_i \frac{p_i^2}{m_i} - gkT\right] \Big/ (gkT\tau_\eta^2) \ .
\end{aligned} \tag{A1}$$

Due to the linear frictions one can derive a reversible centered difference algorithm by expanding the functions to first order; the result is as follows.

From a set of the variables $\mathbf{q}(t), \mathbf{p}(t-h/2), \xi(t-h/2), \eta(t)$ an updated set is obtained after the forces $\mathbf{f}_i(t)$ are calculated as follows:

$$\begin{aligned}
\mathbf{p}_i(t+h/2) &= \{\mathbf{p}_i(t-h/2)[1-\eta(t)h/2] \\
&\quad + h\,\mathbf{f}_i(t)\}/[1+\eta(t)h/2] \ , \\
\eta(t+h) &= \eta(t) + h\left[\sum_i \frac{\mathbf{p}_i(t+h/2)^2}{m_i} - gkT\right] \Big/ (gkT\tau_\eta^2) \ , \\
\xi(t+h/2) &= \xi(t-h/2) \\
&\quad - h\left[\sum_i \mathbf{f}_i(t)\mathbf{q}_i(t) + gkT\right] \Big/ (gkT\tau_\xi^2) \ , \\
\mathbf{q}_i(t+h) &= \frac{\mathbf{q}_i(t)[1-\xi(t+h/2)h/2] + h\,\mathbf{p}_i(t+h/2)/m_i}{1+\xi(t+h/2)h/2} \ .
\end{aligned} \tag{A2}$$

This reversible algorithm is used to integrate the dynamics of the double-well oscillator. The result is shown in Fig. 4.

The Nosé-Hoover (N,P,T) dynamics are obtained from Hamilton's equations by scaling the coordinates $\mathbf{x}^N = \mathbf{q}^N V^{-1/D}$, where V is the volume and D is the dimension, and by introducing a new friction $\zeta(t)$ as follows:

$$\begin{aligned}
&\dot{\mathbf{x}}_i = \mathbf{p}_i/(m_i V^{1/D}) \ , \quad \dot{\mathbf{p}}_i = \mathbf{f}_i - (\dot{\zeta}+\eta)\mathbf{p}_i \ , \\
&\dot{\zeta} = \dot{V}/(DV) \ , \quad \ddot{\zeta} = (P - P_{\rm eq})V/(NkT\tau_\zeta^2)
\end{aligned} \tag{A3}$$

[the dynamics for the T friction $\dot{\eta}$ is unchanged and given by (2)]. The acceleration of the volume friction ζ is given by the excess of the instant pressure $P(t)$ to the external pressure $P_{\rm eq}$ and governed by a characteristic thermostat relaxation time τ_ζ. A leap-frog algorithm for these equations is as follows.

From $\mathbf{x}^N(t)$, $\mathbf{p}^N(t-h/2)$, $V(t)$, $V(t-h)$, $\dot{\xi}(t)$, $\dot{\xi}(t-h)$, and $\eta(t)$ the moments are updated as

$$\mathbf{p}_i(t+h/2) = \frac{\mathbf{p}_i(t-h/2)\{1-[\dot{\xi}(t)+\eta(t)]h/2\}+h\,\mathbf{f}_i(t)}{1+[\dot{\xi}(t)+\eta(t)]h/2} . \tag{A4}$$

The T thermostat friction $\eta(t)$ is updated as in (A2). The volume and the P thermostat parameter ζ as

$$V(t+h)=V(t-h)+2h\dot{\xi}(t)V(t) , \tag{A5}$$

$$\dot{\xi}(t+h)=\dot{\xi}(t-h)+\frac{2h[P(t)-P_{\mathrm{eq}}]V(t)}{NkT\tau_\xi^2} , \tag{A6}$$

where the instant pressure $P(t)$ is

$$DP(t)V(t)=\sum_i^N \frac{\mathbf{p}_i(t+h/2)^2+\mathbf{p}_i(t-h/2)^2}{2m_i} + \mathbf{q}_i(t)\mathbf{f}_i(t) \tag{A7}$$

and finally the coordinates are updated as

$$\mathbf{q}_i(t+h)=\mathbf{q}_i(t)\left[\frac{V(t+h)}{V(t)}\right]^{1/D} + \frac{\mathbf{p}_i(t+h/2)}{m_i}h\left[\frac{2V(t+h)}{V(t+h)+V(t)}\right]^{1/D} . \tag{A8}$$

(In case of an ensemble of molecules only the center of masses are volume scaled.)

The algorithm (A4)–(A8) ensures a time-reversible propagator with pressure fluctuating around P_{eq}.

[1] M. P. Allen and D. J. Tildesley, *Computer Simulation of Liquids* (Oxford University Press, Oxford, 1989).
[2] Wm. G. Hoover, *Computational Statistical Mechanics* (Elsevier, Amsterdam, 1991).
[3] C. Grebogi, S. M. Hammel, J. A. Yorke, and T. Sauer Phys. Rev. Lett. **65**, 1527 (1990).
[4] H. Yoshida, Phys. Lett. A **150**, 262 (1990).
[5] A. Friedman and S. P. Auerbach, J. Comput. Phys. **93**, 171 (1991); **93**, 189 (1991).
[6] E. Forest and R. D. Ruth, Physica D **43**, 105 (1990).
[7] E. Forest, J. Bengtsson, and M. F. Reusch, Phys. Lett. A **158**, 99 (1991).
[8] R. I. McLachlan and P. Atela, Nonlinearity **5**, 541 (1992).
[9] See, however, G. D. Venneri, and W. G. Hoover, J. Comput. Phys. **73**, 468 (1987), J. M. Sanz-Serna, Acta Numer. **1**, 98 (1991).
[10] K. Fox, Celest. Mech. **33**, 127 (1984).
[11] S. Nosé, Mol. Phys. **52**, 255 (1984); W. G. Hover, Phys. Rev. A **31**, 1695 (1985).
[12] B. L. Holian, A. J. DeGroot, W. G. Hoover, and C. G. Hoover, Phys. Rev. A **41**, 4552 (1990).
[13] S. Toxvaerd, Mol. Phys. **72**, 159 (1991).
[14] K. G. Hornell and C. K. Hall, J. Stat. Phys. **61**, 803 (1990).
[15] A. Bulgac and D. Kusnezov, Ann. Phys. (N.Y.) **199**, 187 (1990), D. Kusnezov, A. Bulgac, and W. Bauer, *ibid.* **204**, 155 (1990).
[16] H. A. Posch, W. G. Hoover, and F. J. Vesely, Phys. Rev. A **33**, 4253 (1986).
[17] L. Verlet, Phys. Rev. **159**, 98 (1967).
[18] D. Beeman, J. Comput. Phys. **20**, 130 (1976).
[19] W. C. Swope, H. C. Andersen, P. H. Berens, and K. R. Wilson J. Chem. Phys. **76**, 637 (1982).
[20] M. Tuckerman, B. J. Berne, and G. J. Martyna, J. Chem. Phys. **97**, 1990 (1992).
[21] Energy is in units of ε/k, time in unit of $\sigma(m/\varepsilon)^{1/2}$.
[22] H. J. C. Berendsen and W. F. van Gunsteren, in *Molecular-Dynamics Simulation of Statistical-Mechanical Systems,* edited by G. Ciccotti and W. G. Hoover (North-Holland, New York, 1986), p. 43.
[23] A. Bulgac and D. Kusnezov, Phys. Rev. A **42**, 5045 (1990).
[24] K. Nisizima, Prog. Theor. Phys. **85**, 39 (1991).
[25] S. Toxvaerd, Phys. Rev. B **29**, 2821 (1984); L. F. Rull, J. Morales, and S. Toxvaerd, Phys. Rev. A **38**, 4309 (1988).
[26] E. Fermi, J. Pasta, and S. Ulam, Lect. Appl. Math. **15**, 143 (1974).